

## An evaluation of publicly available global bathymetry grids\*

K. M. Marks\* and W. H. F. Smith

*NOAA Laboratory for Satellite Altimetry, Silver Spring, MD, 20910, USA; \*Author for correspondence (Tel: +1-301-713-2860, ext. 124; Fax: +1-301-713-3136; E-mail: Karen.Marks@noaa.gov)*

Received 30 August 2004, accepted 11 August 2005

**Key words:** bathymetric grids, bathymetry, Coral Sea, DBDB2, ETOPO2, GEBCO, GINA, satellite bathymetry, Woodlark Basin

### Abstract

We evaluate the strengths and weaknesses of six publicly available global bathymetry grids: DBDB2 (Digital Bathymetric Data Base; an ongoing project of the Naval Research Laboratory), ETOPO2 (Earth Topography; National Geophysical Data Center, 2001, ETOPO2 Global 2' Elevations [CD-ROM]. Boulder, Colorado, USA; U.S. Department of Commerce, National Oceanic and Atmospheric Administration), GEBCO (General Bathymetric Charts of the Oceans; British Oceanographic Data Centre, 2003, Centenary Edition of the GEBCO Digital Atlas [CD-ROM] Published on behalf of the Intergovernmental Oceanographic Commission and the International Hydrographic Organization Liverpool, UK), GINA (Geographic Information Network of Alaska; Lindquist et al., 2004), Smith and Sandwell (1997), and S2004 (Smith, unpublished). The Smith and Sandwell grid, derived from satellite altimetry and ship data combined, provides high resolution mapping of the seafloor, even in remote regions. DBDB2, ETOPO2, GINA, and S2004 merge additional datasets with the Smith and Sandwell grid; but moving from a pixel to grid registration attenuates short wavelengths (<20 km) in the ETOPO2 and DBDB2 solutions. Short wavelengths in the GINA grid are also attenuated, but the cause is not known. ETOPO2 anomalies are offset to the northeast, due to a misregistration in both latitude and longitude. The GEBCO grid is interpolated from 500 m contours that were digitized from paper charts at 1:10 million scale, so it is artificially smooth; yet new efforts have captured additional information from shallow water contours on navigational charts. The S2004 grid merges the Smith and Sandwell grid with GEBCO over shallow depths and polar regions, and so is intended to capture the best of both products. Our evaluation makes the choice of which bathymetry grid to use a more informed one.

### Introduction

The world's ocean floors are vast regions covered only sparsely by ship surveys of depth. Only a few percent of the deep ocean floor has been mapped, and the density of ship tracks leaves areas as large as  $10^5 \text{ km}^2$  untraversed. Bathymetry measured indirectly by satellite has been a valuable tool for filling in these unmapped areas, although the extent of coverage is a function of the inclination of the satellite orbit, and the achievable resolution depends on the satellite measurement noise level, and the geologic conditions affecting correlation between satellite-derived gravity anomalies and bathymetric variations.

Efforts to create global bathymetric grids have thus largely involved patching together various

types of data collected at different scales—local ship tracks and multibeam surveys, global satellite bathymetry solutions, and even charts contoured from sparse ship data from both old and more recent surveys, using data collected with ancient to modern navigation techniques. The result is that today, there are at least six global digital bathymetry grids available to choose from. Because each grid uses diverse sources of data that have been combined using varying techniques, and the grid spacing and registration of each grid is different, one grid may be more suitable than another for any given purpose.

This study examines DBDB2 (Digital Bathymetric Data Base; an ongoing project of the Naval Research Laboratory), ETOPO2 (Earth Topography; National Geophysical Data Center, 2001), GEBCO (General Bathymetric Charts of the Oceans; British Oceanographic Data Centre, 2003), GINA (Geographic Information Network

\*The U.S. government right to retain a non-exclusive royalty-free license in and to any copyright is acknowledged.

of Alaska; Lindquist et al., 2004), Smith and Sandwell (1997), and S2004 (Smith, unpublished). We tabulate the various attributes of each global grid, and identify problems, such as grid misregistration, smoothing, data errors, and problems with the methods used to patch different datasets together to form the global grids. We also compare the short wavelength amplitudes that may reflect the fine-scale tectonic details of the seafloor. Our analyses may be used to make an informed choice as to which grid is best for any application.

In our evaluation of these bathymetric grids, we focus on the Woodlark Basin and adjacent Coral Sea area east of Papua New Guinea (Figure 1). This region exhibits a variety of seafloor features, including abyssal hills, seamounts, a plateau, seafloor spreading ridges and fracture zones, and a subduction zone, all within an area small enough to be readily illustrated. Parts of our study area are also covered by a regional scale bathymetry grid (Petkovic and Buchanan, 2002) and a detailed multibeam survey (Goodliffe et al., 1999), facilitating evaluation of each global grid's fidelity to ocean bottom features.

## Bathymetry Grids

Table 1 provides a summary of the attributes of the six global bathymetry grids that we examine. Background information for each of the grids is provided below. We begin with the Smith and Sandwell grid because it is the dataset upon which several other of the bathymetry grids are built.

### *Smith and Sandwell*

Smith and Sandwell (1997) published a 2-min Mercator-projected grid based on bathymetry derived from satellite gravity data, combined with ship measurements. It is possible to map the seafloor from space because marine gravity anomalies reflect the underlying topography. This approach may be advantageous because in most of the ocean, satellite tracks (Figure 2a) sample the gravity field more densely than ship tracks sample bathymetry (Figure 2b–d).

The mathematical details used to derive bathymetry from satellite gravity are published in Smith and Sandwell (1994). A simple summary

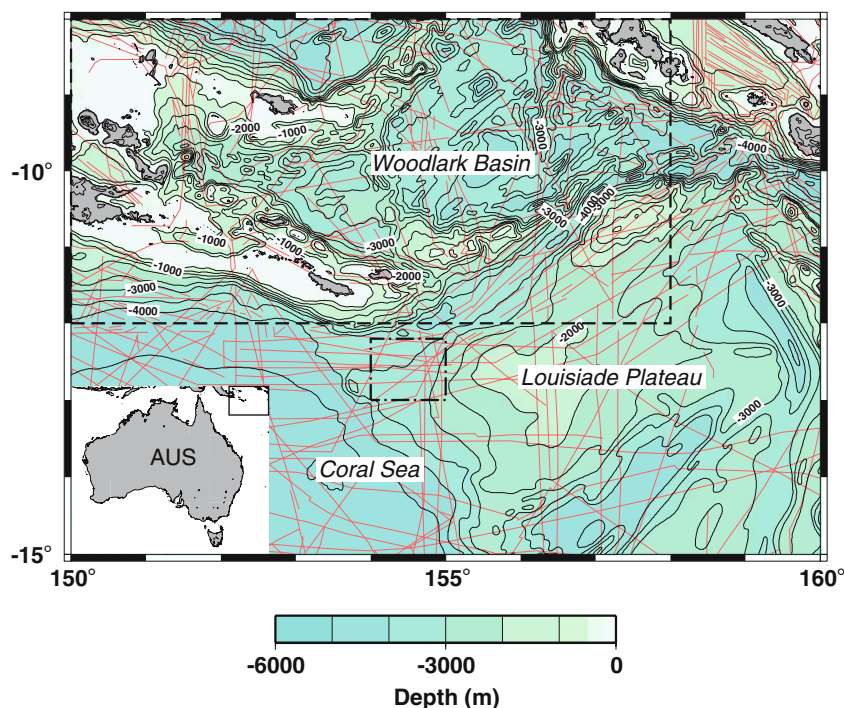


Figure 1. GEBCO contour map of Woodlark Basin study area. Contour interval is 500 m. Dashed region is covered by swath bathymetry in Figure 14. Dash-dot region is enlarged in Figure 12. Red lines are locations of ship tracks used in the GEBCO compilation.

Table 1. Bathymetry grid attributes.

Grid	Spacing	Node	Projection	Coverage	Based on
DBDB2 <sup>a</sup>	2'	grid	geographic	global	Smith and Sandwell <sup>b</sup> below 1000 m depth and between 72° N and 66° S
ETOPO2 <sup>c</sup>	2'	grid	geographic	global	Smith and Sandwell <sup>b</sup> between 64° N and 72° S
GEBCO <sup>d</sup>	1'	grid	geographic	global	Mostly 500 m contours hand-drawn at 1:10 million scale
GINA <sup>e</sup>	30"	pixel	geographic	global	Smith and Sandwell <sup>b</sup> , IBCAO <sup>f</sup> , GTOPO30 <sup>g</sup>
Smith and Sandwell <sup>b</sup>	2'	pixel	Mercator	± 72°	Satellite
S2004 <sup>h</sup>	1'	grid	geographic	global	Smith and Sandwell <sup>b</sup> below 1000 m depth and equatorward of 72°, GEBCO <sup>d</sup> in shallow water and polar regions

<sup>a</sup>NRL (2003); [http://www7320.nrlssc.navy.mil/DBDB2\\_WWW](http://www7320.nrlssc.navy.mil/DBDB2_WWW); we examined both Versions 2.2 and 3.0.

<sup>b</sup>Smith and Sandwell (1997), Version 8.2; [http://topex.ucsd.edu/marine\\_topo/mar\\_topo.html](http://topex.ucsd.edu/marine_topo/mar_topo.html).

<sup>c</sup>NGDC (2001); <http://www.ngdc.noaa.gov/mgg/fliers/01mgg04.html>.

<sup>d</sup>GEBCO (2003); <http://www.bodc.ac.uk/products/gebco.html>.

<sup>e</sup>GINA (2004); <http://www.gina.alaska.edu/page.xml?group=data&page=griddata>.

<sup>f</sup>Jakobsson et al. (2000); <http://www.ngdc.noaa.gov/mgg/bathymetry/arctic/arctic.html>.

<sup>g</sup>USGS (1996); <http://edcdaac.usgs.gov/gtopo30/gtopo30.asp>.

<sup>h</sup>Smith (unpublished); [ftp://falcon.grdl.noaa.gov/pub/walter/Gebco\\_SandS\\_blend.bi2](ftp://falcon.grdl.noaa.gov/pub/walter/Gebco_SandS_blend.bi2).

here is that gravity anomalies are Gaussian filtered to pass full wavelengths < 160 km, and then converted to bathymetry with a gravity-to-topog-

raphy transfer function using appropriate geologic assumptions locally calibrated by ship echo soundings. These predicted bathymetry anomalies are

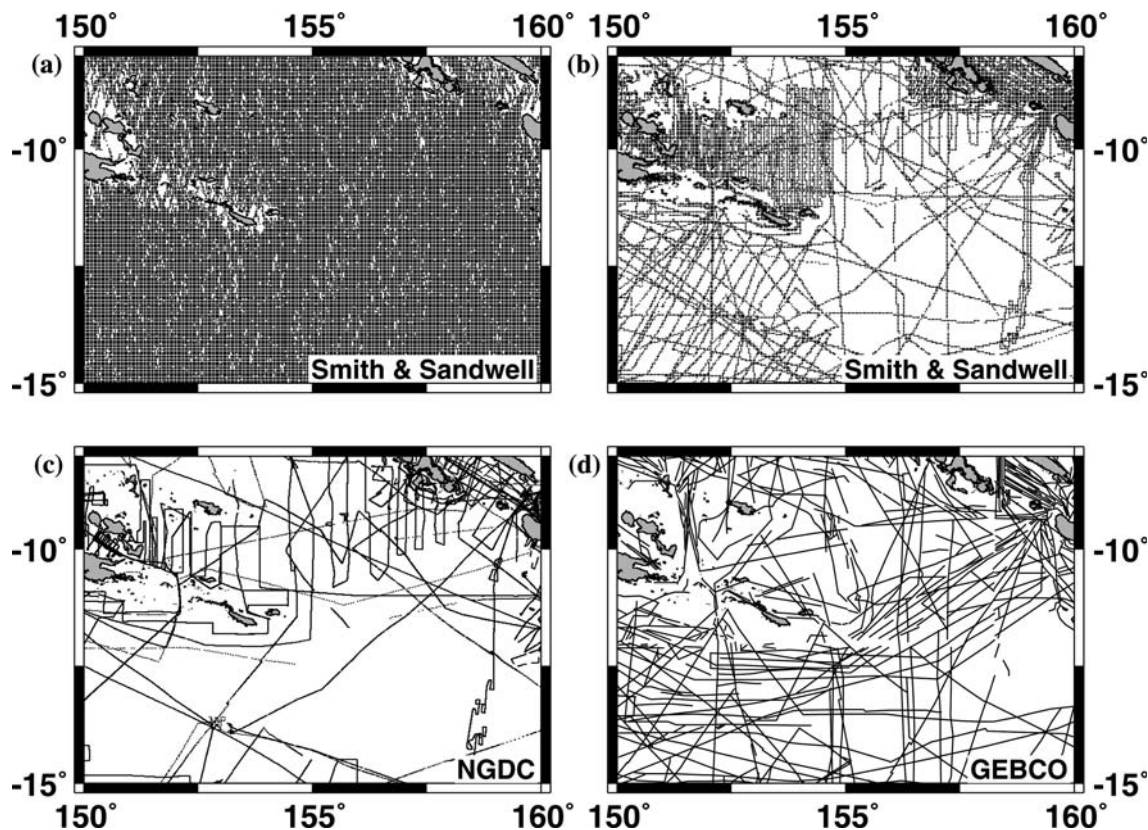


Figure 2. (a) Satellite and (b) ship tracks used in the Smith and Sandwell bathymetry estimation, (c) ship tracks in the NGDC GEODAS database, and (d) ship tracks used in the GEBCO compilation.

then combined with low-pass filtered (passing full wavelengths  $> 160$  km) bathymetric soundings to form the satellite bathymetry grid.

The ship track coverage used by Smith and Sandwell (1997) (Figure 2b) is more complete than is currently available at the National Geophysical Data Center (NGDC) (Figure 2c). Smith and Sandwell were able to obtain ship surveys from investigators to use in their bathymetry solution, but these data are not yet available to the public via the NGDC repository. Over the years, as more ship data became available and as modeling techniques were improved, Smith and Sandwell periodically updated their bathymetric solution. We use the most recent (November, 2000) version 8.2 of the Smith and Sandwell satellite bathymetry grid in our analysis. This grid is shown in Figure 3.

Encoded in this grid are the digital acoustic echo sounding data used to calibrate and constrain the solution. At grid points constrained by ship surveys, the depth value is the median of all soundings nearest the grid point, rounded to the nearest odd integer meter. At grid points estimated from satellite gravity, the depth value is rounded to the nearest even integer meter. This permits users to extract only the constrained points, if desired, as well as to examine the quality and

coverage of the control data (e.g., Figure 2b). This encoding is lost in other grids interpolated from the Smith and Sandwell grid.

### *GEBCO*

The General Bathymetric Charts of the Oceans (GEBCO) grid (British Oceanographic Data Center, 2003; see Table 1) is the only grid we examine that is not based on the Smith and Sandwell grid. It is a 1-min grid that is prepared instead from bathymetric contours of the world's oceans that were originally available as a series of paper maps at 1:10 million scale, and later as digital contours in the GEBCO Digital Atlas. These maps were contoured at 500 m depth intervals, by hand, from both digital and analog ship soundings. The ship track coverage, however, is sparse, irregular, and of uneven quality and navigational control. The red lines in Figure 1 (and also plotted for comparison in Figure 2d) locate ship tracks that GEBCO bathymetrists used to produce the contour map of the Woodlark Basin study area. We do not know the locations or density of the points used to form the contours, but only that those digital (or analog) data points lie along the track lines. These survey tracks are

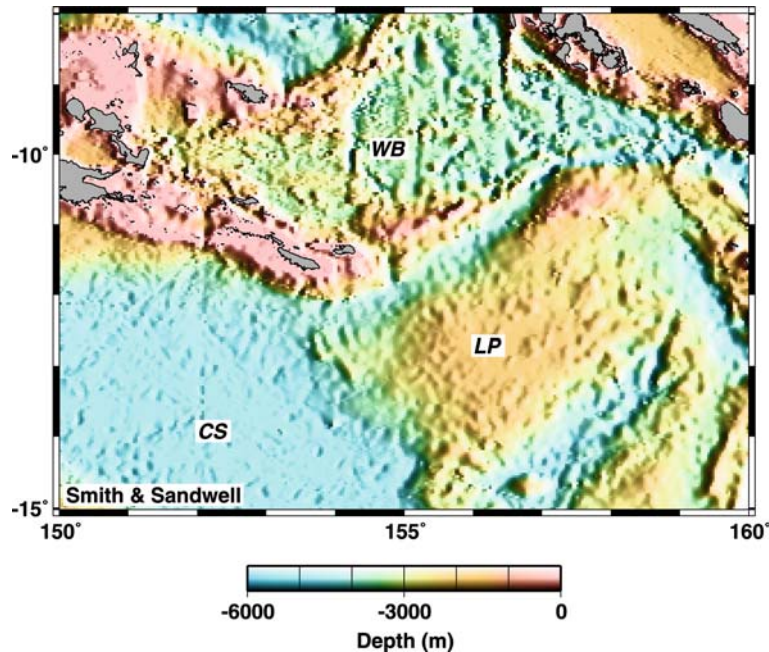


Figure 3. Color shaded-relief image of Smith and Sandwell satellite bathymetry, illuminated from the east. The Woodlark Basin (WB), Coral Sea (CS), and Louisiade Plateau (LP) are labeled here and in subsequent figures.

indicated only as digitized line segments in the GEBCO Digital Atlas. NGDC (National Geophysical Data Center, 2003) ship track coverage (Figure 2c) differs from GEBCO coverage because NGDC's database is digital, and it also contains data from some more recent surveys. We show an image of the GEBCO grid over the Woodlark Basin in Figure 4.

### *ETOPO2*

The ETOPO2 2-min bathymetry grid (Table 1) is a product of the NGDC (National Geophysical Data Center, 2001). It was assembled from the Smith and Sandwell grid between 64° N and 72° S, from the US Naval Oceanographic Office's (NAVOCEANO) Digital Bathymetric Data Base Variable Resolution (DBDBV) data south of 72° S, and from the International Bathymetric Chart of the Arctic Ocean (IBCAO; Jakobsson et al., 2000) data north of 64° N. Land topography is from the GLOBE (GLOBE Task Team et al., 1999) database. Figure 5 is an image of ETOPO2 data in the Woodlark Basin study area.

### *DBDB2*

The Naval Research Laboratory (NRL) at Stennis Space Center in Mississippi produced the DBDB2 2-min bathymetry grid (Table 1). Like ETOPO2, DBDB2 has built upon the Smith and Sandwell satellite bathymetry grid by adding selected regions of higher resolution bathymetric data from Geoscience Australia, IBCAO, Sung Kyun Kwan University, and others to it. There are two versions of DBDB2 available, V2.2 and V3.0 (shown in Figure 6a and b, respectively). Version 3.0 differs from 2.2 in that it has been edited in places by hand, the Smith and Sandwell data were merged with the additional regional datasets at a greater depth, some additional regional data were added, and a different land topography dataset was used (Ko, pers. com., 2004).

### *GINA*

A new attempt to produce a global topography dataset by combining existing grids without a loss in resolution has been undertaken by Lindquist

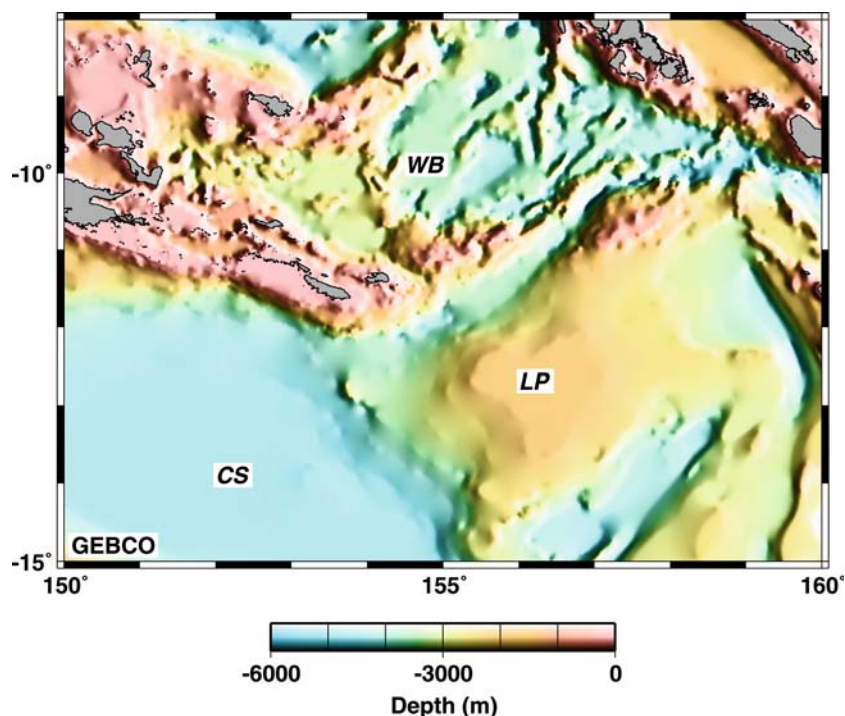


Figure 4. Color shaded-relief image of GEBCO bathymetry, illuminated from the east. Note terraces evident in the image, particularly near the Louisiade Plateau (LP). These result from machine interpolation of digitized contour lines.

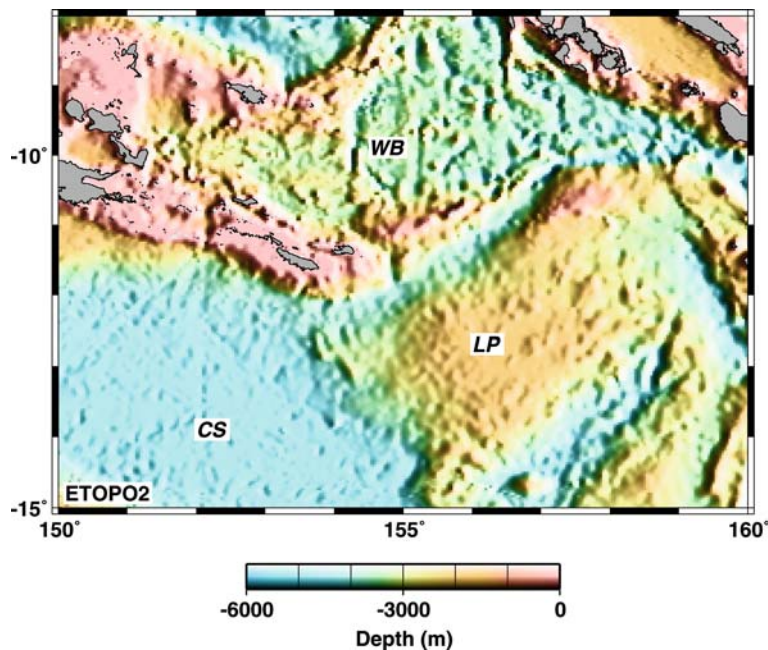


Figure 5. Color shaded-relief image of ETOPO2 bathymetry, illuminated from the east.

et al. (2004). The resulting GINA topography grid (Table 1) was formed by resampling and merging GTOPO30 (US Geological Survey, 1996), Smith and Sandwell, and IBCAO data onto a pixel-registered 30 arc-second grid. The GINA grid over the Woodlark Basin is shown in Figure 7.

#### *S2004*

Walter Smith developed a new 1-min global topography grid (S2004, unpublished; available online, see Table 1) that combines the Smith and Sandwell and GEBCO grids. Smith interpolated the Smith and Sandwell data from its original pixel-registered and Mercator-projected 2-arc-min grid onto GEBCO's grid-registered, geographical, 1-arc-min sampled grid, attempting to preserve all the short-wavelength power present in the Smith and Sandwell grid. Interpolation was by Fourier transform in the east–west direction, resulting in a sinc function interpolant, with an Akima spline used to interpolate from Mercator to geographical spacing in the north–south direction. This resulted in Smith and Sandwell values at full-resolution but on the GEBCO coordinates between  $\pm 72^\circ$  latitude. This was then blended with the GEBCO grid, using GEBCO poleward

of  $72^\circ$  and shallower than 200 m depth (and on land), and Smith and Sandwell equatorward of  $70^\circ$  and deeper than 1000 m depth. Areas in between were smoothly blended with a cosine taper. The result achieves global coverage and one-arc-min geographical coverage, while capturing the seafloor texture of satellite altimetry in deep water areas equatorward of  $70^\circ$ . The S2004 grid over the Woodlark Basin is shown in Figure 8.

#### **Grid Comparisons and Analyses**

##### *Density of Underlying Control Data*

The density of data used to construct a bathymetric grid is an important factor in its resolution – the denser the data, the higher the resolution that can be achieved. Both the GEBCO and the Smith and Sandwell grids include information on the distribution of bathymetric sounding data used to constrain them (Figure 2). The DBDB2, ETOPO2, GINA, and S2004 grids do not convey any information about their control data. However, since they all incorporate the Smith and Sandwell data, we may expect their resolution and characteristics to be similar

to it, except where they have incorporated additional information. We therefore expect the largest overall differences among these grids to be between the GEBCO and the Smith and Sandwell grids.

#### *GEBCO Compared to Smith and Sandwell*

Significant differences between the GEBCO and Smith and Sandwell grids are expected, both because the track control is different (Figure 2)

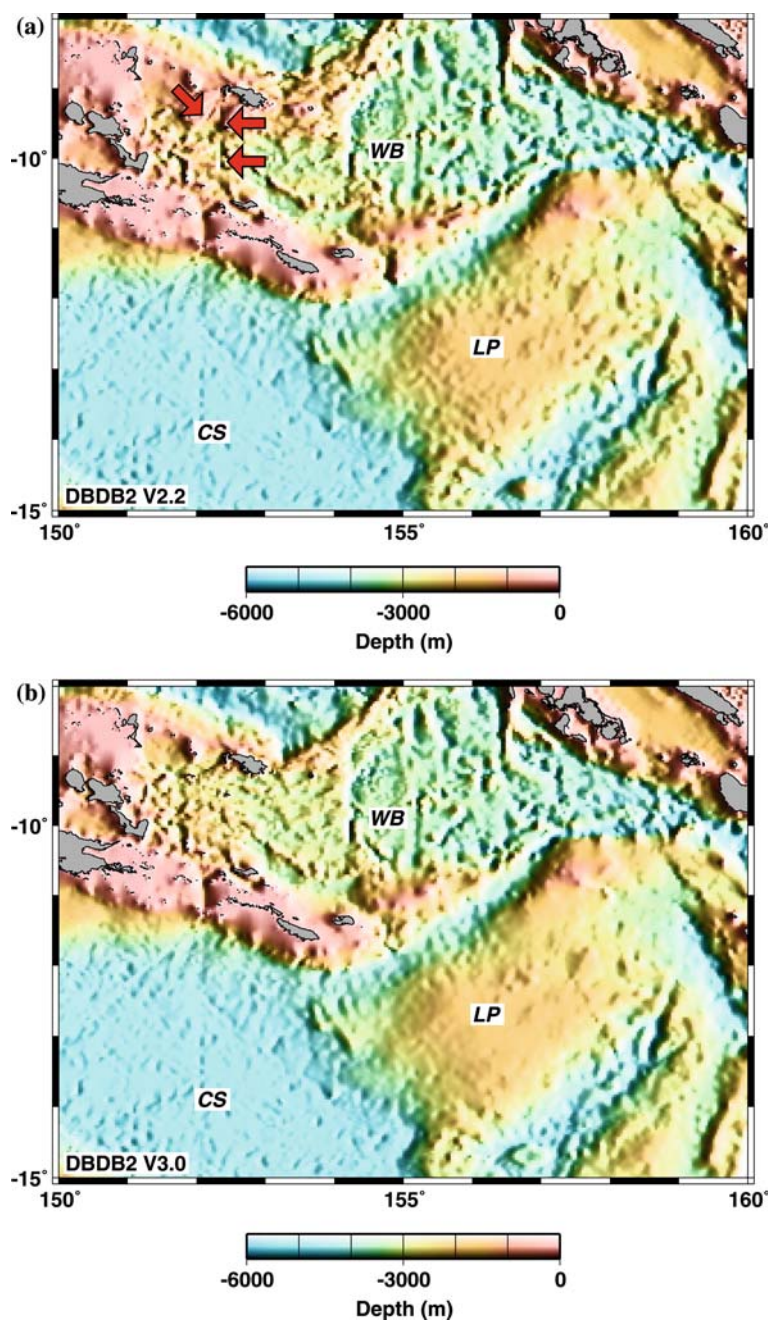


*Figure 6.* (a) Color shaded-relief image of the DBDB2 (Version 2.2) grid and (b) Version 3.0, illuminated from the east. Ship tracks visible in the Australian bathymetry and topography grid (Figure 13) are also present in DBDB2 Version 2.2 (red arrows point to ship tracks), because these data were incorporated.

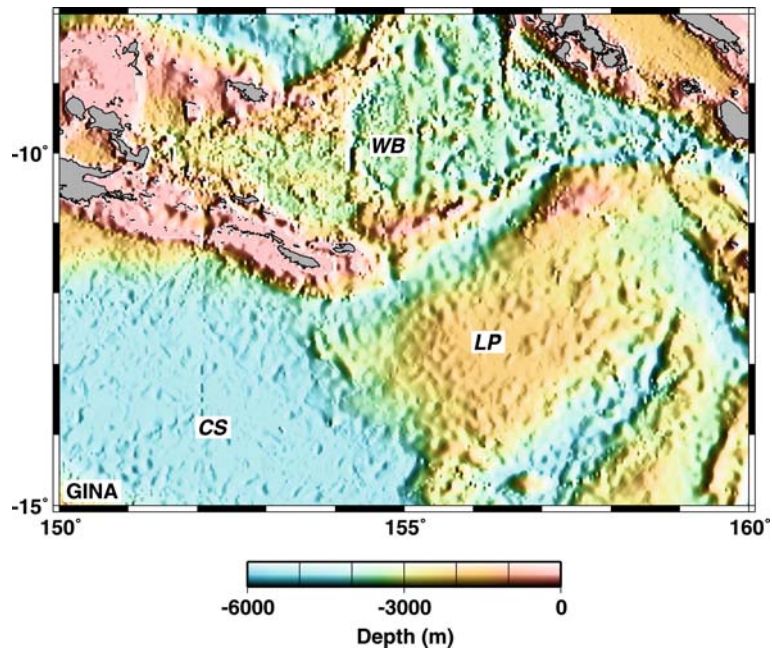


Figure 7. Color shaded-relief image of the GINA grid, illuminated from the east.

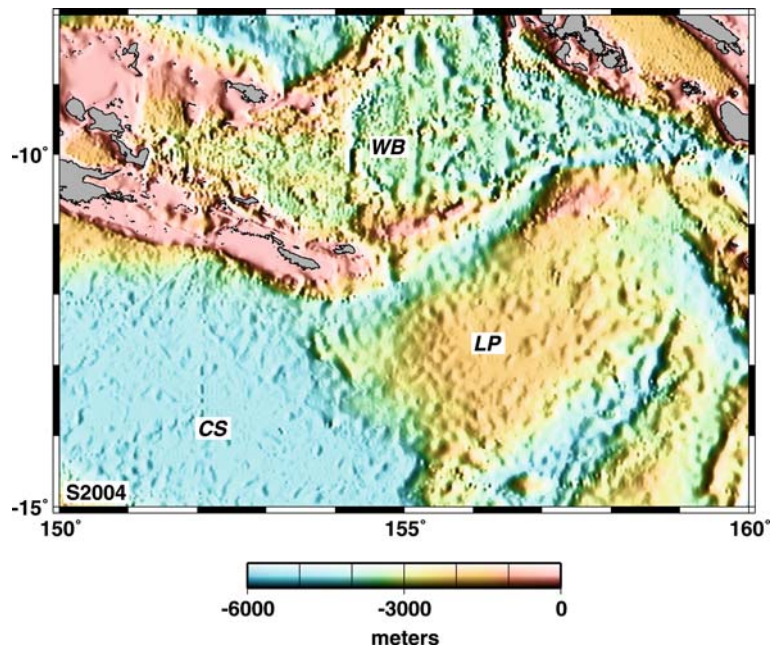


Figure 8. Color shaded-relief image of the S2004 grid, illuminated from the east.

and also because the interpolation between tracks is different: hand-drawn contours versus correlation with gravity. Smith and Sandwell rely on machine interpolation of conventional soundings

to constrain wavelengths greater than about 160 km in their grid, because at longer wavelengths the correlation of gravity with bathymetry may be reduced by isostatic compensation. The

significant differences between the S2004 and GEBCO grids lie chiefly at shorter scales, where the Smith and Sandwell product captures information from satellite gravity. One can remove the gravity-derived information from the Smith and Sandwell grid by low-pass filtering it with the same filter (Gaussian, 160 km full-wavelength at half amplitude) that they use to make the transition between satellite-estimated and ship-constrained wavelength bands (Smith and Sandwell, 1994).

We used this filter to isolate the long-wavelength portions of the GEBCO (Figure 9a) and Smith and Sandwell (Figure 9b) grids, in order to compare them at large scales independent of satellite gravity information. The root-mean-square (RMS) of the differences between these smoothed grids is 119 m, and the mean is 34 m. Figure 9c is an enlargement showing where the differences are  $> 250$  m (green area). This area has ship track control in the Smith and Sandwell grid, but there is no ship track control in the GEBCO grid. We find that, in general, the large-scale features of the two grids are similar, but they may be significantly different where one grid has control data the other lacks.

At shorter spatial scales the two grids also appear very different. In the Smith and Sandwell grid (Figure 3), short-wavelength ( $\sim 20$ – $160$  km) tectonic details of the seafloor in the Woodlark Basin are resolved (e.g., north–south trending lineations along about  $154.1^\circ$  E,  $155.1^\circ$  E, and  $156.4^\circ$  E are fracture zones, and small circular bathymetric highs, e.g., at  $155.5^\circ$  E,  $10.25^\circ$  S and  $155.75^\circ$  E,  $9.75^\circ$  S, are seamounts). The pervasive “bumpy” background fabric, while due in part to noise in the altimeter data, may also be related to small-scale morphology of the ocean floor (Goff et al., 2004).

Even though the GEBCO grid spacing is 1-min, it has a generally smooth appearance (Figure 4), and neither the bumpy fabric nor the above tectonic details are evident. The GEBCO grid is derived primarily from digitized 500 m contours drawn at 1:10 million scale. At this scale, contours can only be drawn about 3 mm apart. Thus the map scale alone limits the horizontal resolution to about 30 km, and the slope of the ocean floor to about 1 degree. The map scale also limits the vertical resolution – for example, abyssal hills will not be detected because their maximum relief is only 300 m (Goff, 1991). The contours appear as terraces in the GEBCO grid and are particularly

visible around the Louisiade Plateau (see Figure 4).

These terraces cause spikes in the histogram of GEBCO depths to appear at contour values (Figure 10a). In contrast, the distribution of depths in the Smith and Sandwell grid (Figure 10b), displays a smooth distribution of

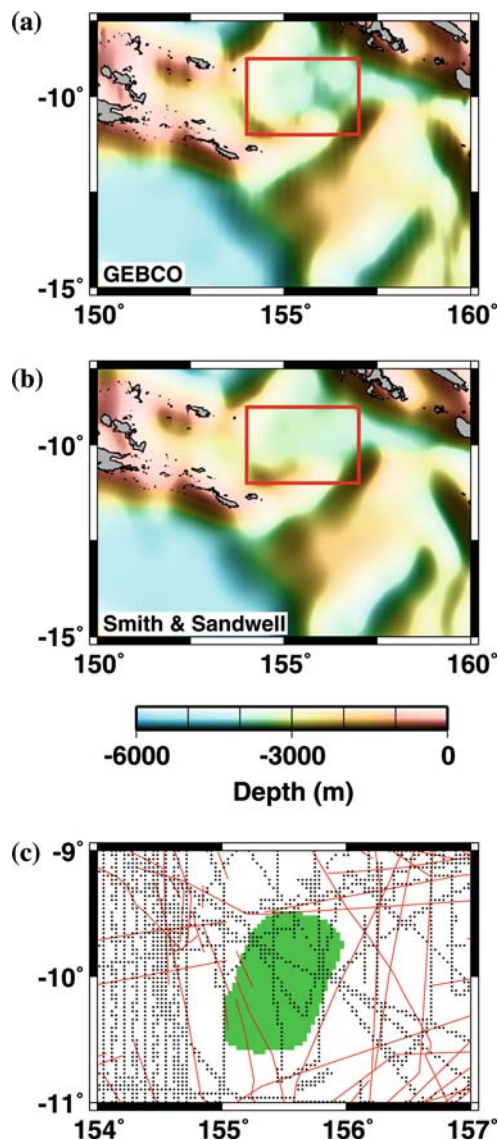


Figure 9. Low-pass (wavelengths  $> 160$  km) filtered bathymetry from (a) GEBCO and (b) Smith and Sandwell. The RMS of the difference between the two low-pass fields is 119 m, and the mean difference is 34 m. The red box in (a) and (b) is enlarged in (c). (c) Smith and Sandwell ship control points (black dots) cover the region where differences are  $> 250$  m (green area), but GEBCO ship tracks (red lines) do not, indicating this seafloor high is not detected in the GEBCO grid.

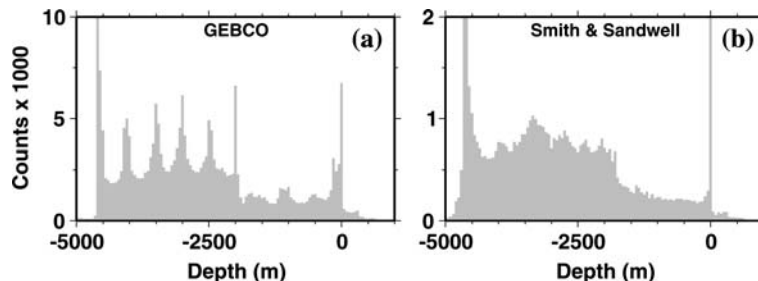


Figure 10. Histograms of (a) GEBCO depths and (b) Smith and Sandwell depths, at a bin width of 50 m. The GEBCO depths (a) spike at the 500 m contour values. The spike at 4500 m in the Smith and Sandwell grid reflects flat sediments in the southwestern portion of the study area, while the spike at 0 m reflects the use of a high-resolution land-sea boundary.

depths except for spikes at 4500 and 0 m. A region of flat sediments in the Coral Sea (southwest portion of the study area, see Figure 3) accounts for the large number of 4500 m depths. The spike at 0 m occurs because Smith and Sandwell constrained the land-sea boundary in their grid with the high-resolution World Vector Shoreline (Wessel and Smith, 1996).

#### *Registration, Sampling, Interpolation and Smoothing*

We turn now to compare Smith and Sandwell to the other grids in our study, which have incorporated it (DBDB2, ETOPO2, GINA, S2004). Smith and Sandwell’s original product is given on a Mercator-projected and pixel-registered coordinate system, but all the other grids have interpolated it onto meshes having equidistant sampling in longitude and latitude (not Mercator-projected). One immediate consequence of this interpolation is that the encoding of the location of control soundings was lost. In this section and the next we examine some additional consequences.

The particular coordinate system used by Smith and Sandwell (1997) facilitated their work. Their calculations required a conformal map projection. Among conformal projections, the Mercator was a good choice because its increasing magnification of area at increasing latitude counteracts the increasing spatial density of the satellite ground tracks, effectively spreading the data out more nearly uniformly. Having chosen to compute the solution in Mercator map coordinates, it then made sense to use a pixel registration so that imaging software could plot maps directly without further interpolation.

However, care must be exercised when interpolating between grid meshes, lest fine-scale information be lost. Figure 11a demonstrates what happens when the 2-arc-min pixel-registered mesh of Smith and Sandwell is resampled onto a 2-arc-min grid-registered mesh such as used in DBDB2 and ETOPO2. In this interpolation, the original data are sampled on meridians at odd-numbered minutes of longitude, and the derived data are sampled on meridians at even-numbered minutes of longitude. The Nyquist wavelength of the original mesh is a waveform with amplitudes of 1 and  $-1$  at odd arc-minutes. If this waveform is sampled at even arc minutes the waveform vanishes.

More generally, at wavelengths longer than the Nyquist wavelength, amplitudes will also be attenuated, though they will not go entirely to zero. The amplitude loss in going from the Smith and Sandwell grid to the DBDB2 or ETOPO2 grid is  $\cos(2\pi/\lambda)$ , where  $\lambda \geq 4$  is the wavelength in arc-minutes. This transfer function, as a function of wavelength, is shown in Figure 11b. The DBDB2 and ETOPO2 grids should be smoother than the original Smith and Sandwell grid, at least in areas where they have resampled it without incorporating any new information.

The ETOPO2 grid in the Woodlark Basin (Figure 5) looks very similar to the Smith and Sandwell grid (Figure 3), because ETOPO2 is based on the Smith and Sandwell grid at these latitudes. Closer inspection, however, reveals a slightly smoother appearance to the ETOPO2 grid – for example, note how the fracture zones and seamounts are not as crisp. This smoothing results from NGDC’s interpolation of the pixel-registered Smith and Sandwell grid onto a grid-registered ETOPO2 grid. Like ETOPO2, DBDB2 (V2.2 and

V3.0, Figure 6a and b) was interpolated from Smith and Sandwell bathymetry onto a grid-node registration, so it demonstrates the same smoothing as a result.

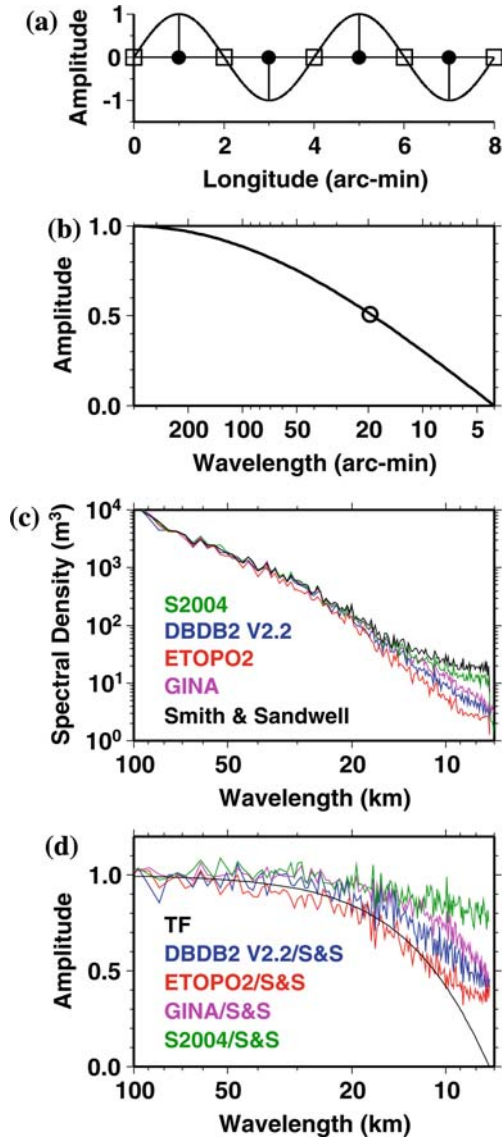


Figure 11. (a) The Nyquist wavelength of the 2-arc-min, pixel-registered Smith and Sandwell grid has local maxima and minima at odd meridians (black circles) and zero crossings at even meridians (open squares), where DBDB2 and ETOPO2 are sampled. (b) The transfer function for moving between odd (pixel) and even (grid) 2-arc-min registrations. At a wavelength of 20 arc-min ( $\sim 36$  km at  $11.5^\circ$  N), the amplitude is reduced by half. (c) The spectral density of the grids based partly on satellite altimetry is similar at long wavelengths but significantly different at wavelengths shorter than 20 km. (d) The spectrum of amplitude ratios for the other grids with respect to Smith and Sandwell, compared to the theoretical pixel-to-grid transfer function (TF).

### Spectral Analyses

Figure 11c plots the spectral density of each of the grids incorporating altimetry. The attenuation caused by moving from a pixel to a grid registration is exhibited as a reduction of power at wavelengths shorter than about 20 km for ETOPO2 and DBDB2, as compared to Smith and Sandwell. Although we plot only the spectrum for DBDB V2.2, V3.0 has a similar loss in power. The spectral density of the S2004 grid is slightly lower at shorter wavelengths than for Smith and Sandwell. This is because, in shallow water, the smoother GEBCO data were added to the S2004 solution.

Even though the GINA grid is sampled on a pixel-registered grid that includes the original Smith and Sandwell points, it still exhibits a reduction in power at shorter wavelengths (Figure 11c). Discussions with one of the authors (Engle, pers. com., 2005) about the details of how the GINA grid was constructed did not reveal any reason for the cause of the attenuation. There was no filtering when the 2 min Sandwell and Smith grid was resampled onto a 30 arc-second grid. This leaves us to speculate the attenuation may be due to the bilinear or bicubic interpolation used in the resampling.

We note that both the Smith and Sandwell and S2004 power spectra appear to flatten out at wavelengths shorter than about 15 km (Figure 11c). This flattening may be the signature of white noise in the altimeter data. The power spectra for the other grids do not flatten out, but instead maintain the spectral slope to shorter wavelengths. For the ETOPO2 and DBDB2 spectra, this can be a result of noise (along with short wavelength signal) being smoothed out due to moving to a grid registration. This is not necessarily a bad thing, if noise suppression is preferred over seafloor fabric resolution.

In Figure 11d we divide the amplitude spectra of the different grids by the Smith and Sandwell amplitude spectrum, and compare that ratio to the transfer function for moving between a pixel and a grid registration. In this way we can visualize the amplitude loss at different wavelengths due to changing the grid registration. The transfer function models the ratio of ETOPO2/Smith and Sandwell well at wavelengths  $> 10$  km, demonstrating how the loss of amplitudes in the ETOPO2

grid is mostly a result of changing the grid registration. The DBDB2/Smith and Sandwell amplitudes are higher than those of the transfer function at shorter ( $< 20$  km) wavelengths. This is due to the higher-resolution Australian bathymetry and topography data incorporated into the DBDB2 grid in our study area. It is possible that the amplitudes of the GINA/Smith and Sandwell curve are higher than those of the transfer function because the 30 arc-second GTOPO30 land data may have been incorporated in the GINA grid covering our Woodlark Basin study area. Finally, the amplitudes of S2004/Smith and Sandwell are slightly less than one (approaching .85 at 10 km wavelength) at shorter wavelengths. This demonstrates how the short wavelength power of Smith and Sandwell is retained in the S2004 grid, but is slightly lowered by the incorporation of GEBCO data.

## Grid Problems

### *Mislocation of ETOPO2*

In addition to the smoothing effect of interpolation, there is also the possibility that mistakes may

be introduced in registration of the data. It appears that the data in ETOPO2 are misregistered in latitude and longitude. This occurred while the global grid was being assembled from its major components at NGDC. We demonstrate the systematic offset in Figure 12a. The black lines contour the Smith and Sandwell grid over an enlarged area in the Coral Sea (dash-dot outlined in Figure 1). The red lines contour ETOPO2 bathymetry anomalies, which are systematically offset to the northeast.

This shift in location is not a necessary consequence of the movement from the Smith and Sandwell grid mesh to the ETOPO2 grid mesh, as DBDB2 has the same sampling as ETOPO2 but does not show this error (Figure 12b). The GINA and S2004 grids also did not make this mistake.

### *Other Grid Problems*

Here we note other problems observed in the grids, which range from incorrectly merging ship data into a grid, to mixing bad data with good, to imperfections created when patching together adjacent datasets.

Red arrows in Figure 6a point to ship tracks that are evident in the DBDB2 V2.2 bathymetry

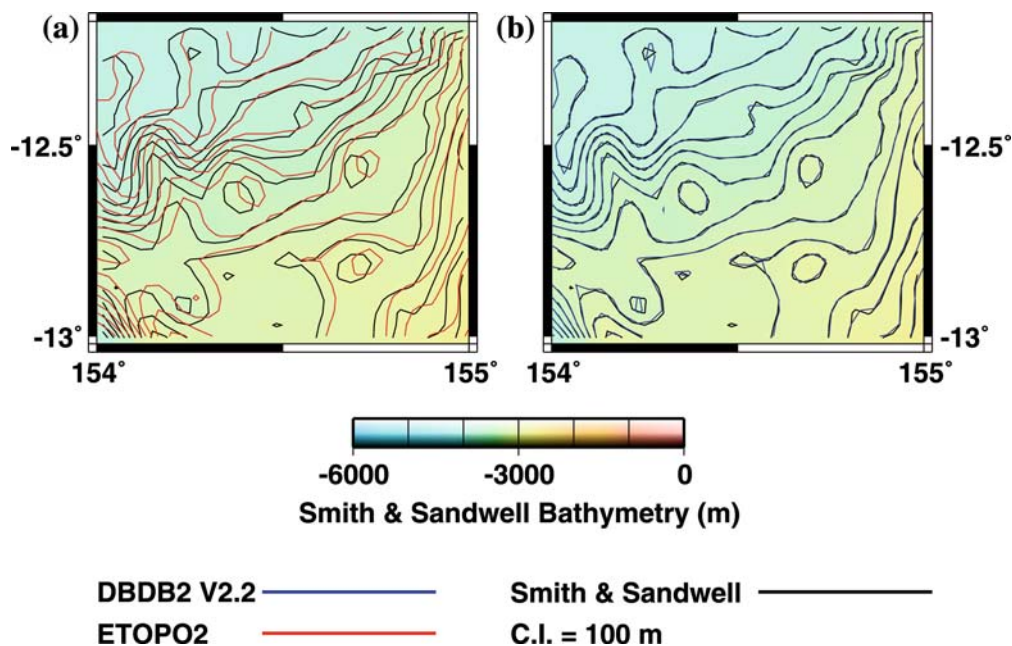


Figure 12. Smith and Sandwell satellite bathymetry overlain by (a) ETOPO2 contours and (b) DBDB2 contours. The registration offset to the northeast is seen in the ETOPO2 contours. DBDB2 contours are correctly registered.

anomalies. These tracks result from ship track soundings being incorrectly merged into the bathymetry grid. Regional data from the Australian bathymetry and topography grid (Petkovic and Buchanan, 2002) (Figure 13) that were incorporated into the DBDB2 solution show the same ship tracks, so these imperfect data were simply ingested into DBDB2.

We obtained detailed swath bathymetry data covering the Woodlark Basin (Goodliffe et al., 1999) (Figure 14). It appears that the western portion of the detailed swath bathymetry survey was incorporated into the Australian bathymetry and topography grid (compare Figures 13 and 14). Yet the detailed swath bathymetry data do not contain the ship tracks that are evident in DBDB2 V2.2 and the Australian bathymetry and topography grids.

We show DBDB2 V3.0 (Figure 6b) to demonstrate that grids evolve, solving some problems but possibly introducing others. In V3.0 an attempt was made to remove, via hand-editing, the bad ship tracks in the western Woodlark Basin from the Australian bathymetry and topography data prior to incorporation into the DBDB2 solution. However, the transition between Smith and Sandwell and Australian data occurs at a greater

depth in V3.0 (Ko, pers. com., 2004), causing shallower topography to be smoother than in V2.2, in regions not covered by the detailed swath bathymetry (note the smoother appearance of the seafloor on the flanks of the Louisiade Plateau).

The higher resolution swath bathymetry data do not improve the DBDB2 solutions much because they are decimated when gridded at a 2-min spacing. We note the fracture zones and seamounts that are resolved in the Smith and Sandwell grid are very clear in the swath bathymetry.

In places, the Smith and Sandwell grid displays bad ship tracks (inside red circle in Figure 15). These occur where ship bathymetry data are too poor to be successfully incorporated into the gridded bathymetry solution. Future versions of the Smith and Sandwell bathymetry solution will omit these bad tracks. When such features lie in water deeper than 1000 m and equatorward of 70°, the same errors should appear in the S2004 grid.

In the GEBCO grid, regions were interpolated separately and then combined to form the global grid. Seams may show up where some of these regions were patched together. Two such seams are evident southeast of our study area (red arrows point to seams in Figure 15).

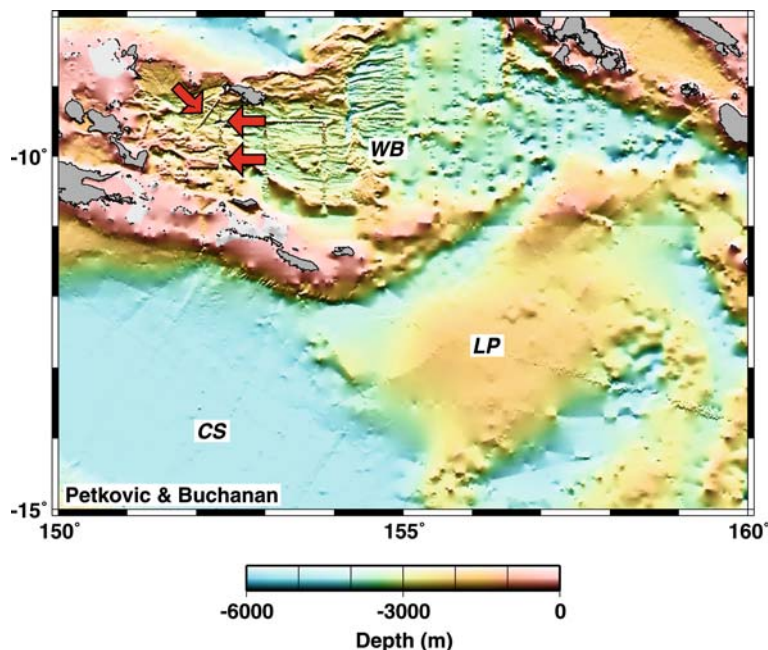


Figure 13. Color shaded-relief image of the Australian bathymetry and topography grid (Petkovic and Buchanan, 2002), “illuminated” from the north. Red arrows point to ship tracks visible in grid.

The tectonic features of the seafloor mapped by the GEBCO grid may appear different in extent and shape than they actually are. An example of this is shown in Figure 16a, where the Smith and Sandwell topography grid maps the northwest–southeast trending Foundation Seamount Chain (Mammerickx, 1993), while the GEBCO grid displays an east–west trending seamount chain

(Figure 16b). This occurs because only seamounts and troughs traversed by ship tracks are detected, so only these detected features are mapped by the grid. However, most seamounts are missed because they lie between ship tracks (Figure 16c). A trough is likewise not detected in the GEBCO grid, yet is clearly mapped as a northwest–southeast trending trough in the Smith and Sandwell grid.

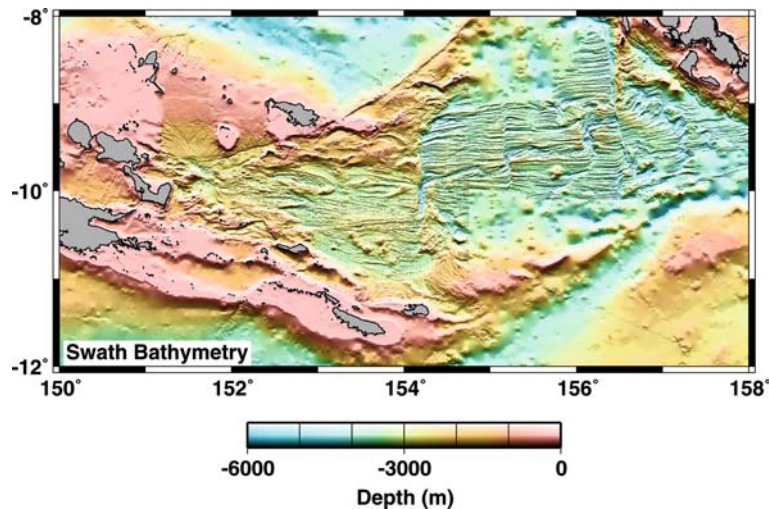


Figure 14. Color shaded-relief image of swath bathymetry in the Woodlark Basin (Goodliffe et al., 1999). The image is “illuminated” from the north.

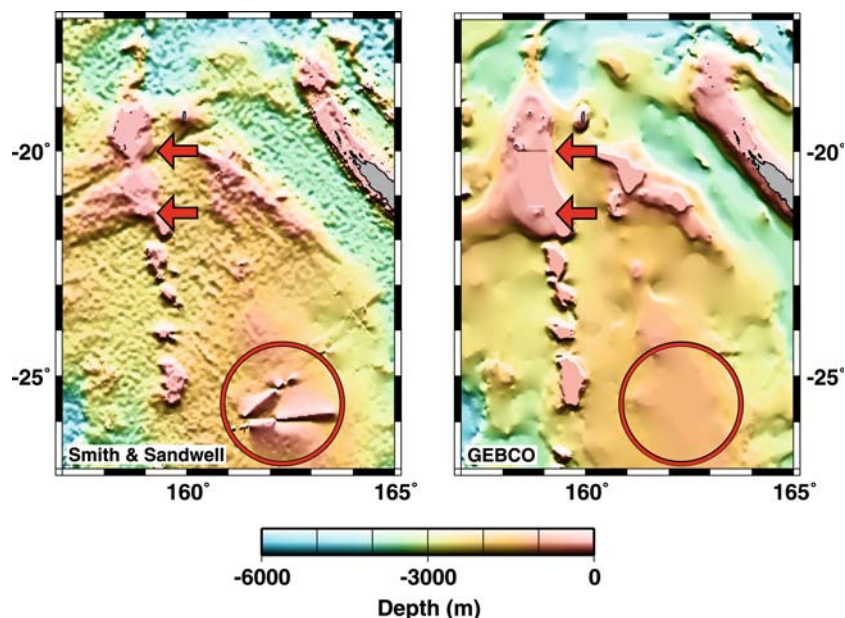


Figure 15. Some bad ship tracks (circled) are present in the Smith and Sandwell grid, that are not in the GEBCO grid. Seams, due to patching together individually interpolated regions, are present in the GEBCO grid (red arrows point to seams) that are not in the Smith and Sandwell grid.

## Concluding Remarks

Our comparison of six bathymetric grids reveals that for many marine geoscience purposes, the original Smith and Sandwell grid may be the best choice. Both the DBDB2 and ETOPO2 grids, which are based on the Smith and Sandwell grid, in fact degrade the solution by interpolating it onto a grid registration. The resulting loss in short-wavelength information blurs sharp features such as tectonic lineaments and seamount summits. Some of the higher-resolution regional surveys ingested into the DBDB2 solutions contain errors. We have also determined that the GINA grid has been smoothed, but the construction steps do not reveal the reason.

ETOPO2 is also problematic because it is misregistered in latitude and longitude. For some users, the mislocation of features in ETOPO2 will be the most serious issue discussed in this paper.

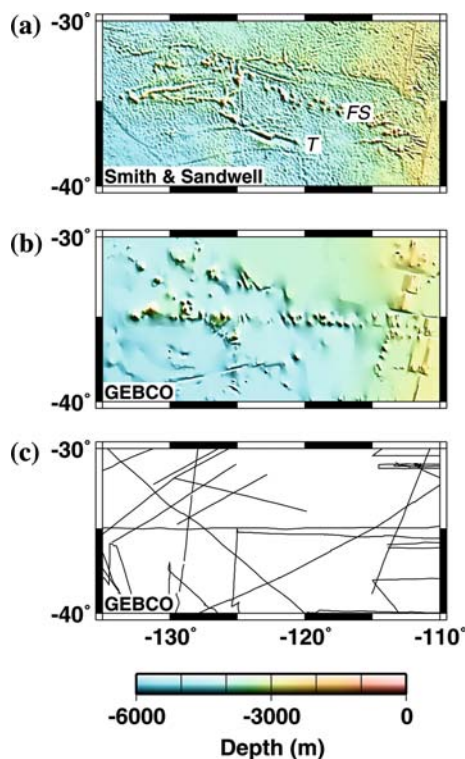


Figure 16. (a) The northwest–southeast trending Foundation Seamount chain (FS) and an unnamed trough (T) are well resolved in the Smith and Sandwell grid. Only seamounts and troughs traversed by ship tracks (c) show up in the GEBCO grid (b). Most seamounts in the GEBCO grid are missed because they lie between ship tracks, and seamounts that are traversed by ship tracks appear aligned along the tracks, rather than in their true orientation.

For researchers who prefer a 1-min geographic grid with global coverage, S2004 is a good choice. An advantage of the original Smith and Sandwell grid, however, is that it encodes the sounding control information. This allows the user to map the control locations, or to extract only the measured values and throw away the interpolated ones, if desired. This encoding is lost in all the grids interpolated from Smith and Sandwell, including ETOPO2, DBDB2, GINA, and S2004.

An advantage of the S2004 grid is that it is on a geographic grid, which users may find convenient. Satellite altimeter track coverage can be spotty near land (see Figure 2a) and altimetry is poorly correlated with bathymetry in shallow coastal areas. In some parts of the world the GEBCO grid production team put new effort into capturing information from shallow water contours on navigational charts. For these reasons, the GEBCO grid may be superior to Smith and Sandwell in some shallow water areas. S2004 attempts to capture the best information from both products. For purposes of displaying smooth 500 m bathymetric contours, the GEBCO grid is a good choice. Contours of the Smith and Sandwell grid are jagged because of the noise contained in the solution. This noise (along with some signal) shows up as a bumpy background texture in the Smith and Sandwell grid, and some users may want to smooth this.

Future versions of DBDB2 and ETOPO2 can be improved by honoring the pixel registration of the underlying Smith and Sandwell grid. The Smith and Sandwell grid can be improved by making a new solution that incorporates more recent ship data and high-resolution regional and local surveys. It would be more user-friendly, too, if it were made available in a geographic grid. A new satellite mission capable of collecting higher-resolution altimetry data would yield a greatly improved bathymetry solution containing significant new details. Extending the bathymetry solution to latitudes higher than 72°, as in the S2004 solution, would be desirable.

## Acknowledgements

We thank Eric Bayler for suggesting we look at DBDB2. John Goff and David Caress provided helpful reviews that improved the manuscript.

The following researchers kindly provided us with data: Dong-Shan Ko of NRL provided DBDB2 Versions 2.2 and 3.0, and Andrew Goodliffe, Fernando Martinez, and Brian Taylor of the School of Ocean and Earth Science and Technology, University of Hawaii, provided swath bathymetry in the Woodlark Basin. Kevin Engle was very helpful discussing the construction of the GINA grid. Graphics were created using the Generic Mapping Tools (GMT) software package (Wessel and Smith, 1998). The views, opinions, and findings contained in this report are those of the authors and should not be construed as an official National Oceanic and Atmospheric Administration or US Government position, policy, or decision.

## References

- British Oceanographic Data Centre, 2003, *Centenary Edition of the GEBCO Digital Atlas [CD-ROM]*. Liverpool, UK: Published on behalf of the Intergovernmental Oceanographic Commission and the International Hydrographic Organization.
- GLOBE Task Team and Hastings, D.A., Dunbar, P.K., Elpingstone, G.M., Bootz, M., Murakami, H., Maruyama, H., Masaharu, H., Holland, P., Payne, J., Bryant, N., Logan, L., Muller, J.-P., Schreier, G. and MacDonald, J.S., 1999, The Global Land One-kilometer Base Elevation (GLOBE) Digital Elevation Model, Version 1.0. National Oceanic and Atmospheric Administration, National Geophysical Data Center, 325 Broadway, Boulder, Colorado, USA.
- Goff, J.A., 1991, A global and regional stochastic analysis of near-ridge abyssal hill morphology, *J. Geophys. Res.* **96**, 21713–21737.
- Goff, J.A., Smith, W.H.F. and Marks, K.M., 2004, The contributions of abyssal hill morphology and noise to altimetric gravity fabric, *Oceanography* **17**, 24–37.
- Goodliffe, A., Taylor, B. and Martinez, F., 1999, Data Report: Marine geophysical surveys of the Woodlark Basin region, in Taylor, B., Huchon, P., Klaus, A., et al. (Eds.), *Proceedings of the Ocean Drilling Program, Initial Reports*, 180, pp. 1–20 [CD-ROM]. Ocean Drilling Program, Texas A&M University, College Station, Texas, USA.
- Jakobsson, M., Cherkis, N.Z., Woodward, J., Macnab, R. and Coakley, B., 2000, New grid of Arctic bathymetry aids scientists and mapmakers, *EOS, Trans. Am. Geophys. Union* **81**, 89–96.
- Lindquist, K.G., Engle, K., Stahlke, D. and Price, E., 2004, Global topography and bathymetry grid improves research efforts, *EOS, Trans. Am. Geophys. Union* **85**, 186.
- Mammerickx, J., 1993, The foundation seamounts: tectonic setting of a newly discovered seamount chain in the South Pacific, *Earth Planetary Sci. Lett.* **113**, 293–306.
- National Geophysical Data Center, 2001, *ETOPO2 Global 2' Elevations [CD-ROM]*. Boulder, Colorado, USA: U.S. Department of Commerce, National Oceanic and Atmospheric Administration.
- National Geophysical Data Center, 2003, *Worldwide Marine Geophysical Data, GEODAS Version 4.1.18 [CD-ROM]*. Boulder, Colorado, USA: Data Announcement 2003-MGG-02, U.S. Department of Commerce, National Oceanic and Atmospheric Administration.
- Petkovic, P. and Buchanan, C., 2002, *Australian Bathymetry and Topography Grid [digital dataset]*. Canberra, Australia: Geoscience Australia.
- Smith, W.H.F. and Sandwell, D.T., 1994, Bathymetric prediction from dense satellite altimetry and sparse shipboard bathymetry, *J. Geophys. Res.* **99**, 21803–21824.
- Smith, W.H.F. and Sandwell, D.T., 1997, Global sea floor topography from satellite altimetry and ship depth soundings, *Science* **277**, 1956–1962.
- U. S. Geological Survey, 1996, *Global 30 Arc-Second Elevation Data Set (GTOPO30)*. EROS Data Center. Sioux Falls, South Dakota, USA: Land Processes Distributed Active Archive Center.
- Wessel, P. and Smith, W.H.F., 1996, A global self-consistent hierarchical high-resolution shoreline database, *J. Geophys. Res.* **101**, 8741–8743.
- Wessel, P. and Smith, W.H.F., 1998, New, improved version of Generic Mapping Tools released, *EOS, Trans. Am. Geophys. Union* **79**, 579.